NANO LETTERS

Letter

pubs.acs.org/NanoLett

Roll-to-Roll Transfer of Electrospun Nanofiber Film for High-Efficiency Transparent Air Filter

Jinwei Xu,[†] Chong Liu,[†] Po-Chun Hsu,[†] Kai Liu,[†] Rufan Zhang,[†] Yayuan Liu,[†] and Yi Cui*[,†,‡]

[†]Department of Materials Science and Engineering, Stanford University, Stanford, California 94305, United States

[‡]Stanford Institute for Materials and Energy Sciences, SLAC National Accelerator Laboratory, 2575 Sand Hill Road, Menlo Park, California 94025, United States

Supporting Information

ABSTRACT: Particulate matter (PM) pollution in air has become a serious environmental issue calling for new type of filter technologies. Recently, we have demonstrated a highly efficient air filter by direct electrospinning of polymer fibers onto supporting mesh although its throughput is limited. Here, we demonstrate a high throughput method based on fast transfer of electrospun nanofiber film from roughed metal foil to a receiving mesh substrate. Compared with the direct electrospinning method, the transfer method is 10 times faster and has better filtration performance at the same transmittance, owing to the uniformity of transferred nanofiber film (>99.97% removal of $PM_{2.5}$ at ∼73% of transmittance). With these advantages, large area freestanding nanofiber film and roll-to-roll production of air filter are demonstrated.

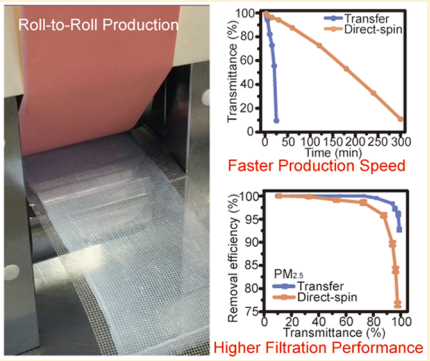

KEYWORDS: *Electrospinning, roll-to-roll, transfer, transparent, air filter, $PM_{2.5}$*

Particulate matter (PM) pollution in air has recently become one of the most serious environmental issues that poses huge threat to public health.[1,2] PM is a complex mixture of small solid particles and liquid droplets. According to size, PM can be categorized by $PM_{2.5}$ and PM_{10}, representing particle sizes below 2.5 and 10 μm, respectively.[3] $PM_{2.5}$ is particularly harmful since its size is small enough to penetrate the human lungs and go into the body circulation system.[4] Long-term exposure to PM pollution can lead to heart disease, strokes, and lung disease, including cancer.[5−9] While short-term exposure to high concentration of PM can trigger asthma attacks. Due to its severe impact on public health,[10] it is necessary and urgent to deploy effective protection for the public from present hazy days.[11,12] Some efforts have been made toward outdoor individual protection[13,14] and modern commercial building protection.[15−17] The essential component of PM removal technology is the filtration membrane.[18] Ideally, the air filter should have high air flux with low resistance yet high PM filtration efficiency. In our previous work,[19] we have demonstrated that polar polymer nanofibers such as polyacrylonitrile (PAN) have much stronger affinity to PM pollutants than the nonpolar polypropylene fibers used in the existing filtration membrane. The high capture efficiency of the polar polymer nanofiber membrane makes it possible to use thin nanofiber membrane on a supporting grids and to have good optical transparency and low air flow resistance. Such an efficient nanofiber membrane opens up the opportunities to be used not only for personal masking and building ventilation filtering, but also as transparent window screen under natural ventilation.

Our previous transparent filters were fabricated by electrospinning of polymer nanofibers directly onto a conducting mesh (Figure 1a). While nanofibers offer the PM capture function, the macroscale mesh provides stable mechanical support to nanofiber membrane. This macroscale mesh needs to be electrically conducting in order to maintain the normal electrospinning process. However, the conducting mesh geometry creates highly nonuniform electric field distribution across the whole surface (much stronger directly on mesh grids), resulting in the corresponding nonuniform deposition of polymer nanofibers. Polymer nanofibers would accumulate much more on the metallic lines of mesh, and the number density is much less on the empty space between the metallic lines. This can be clearly seen on the bright field optical microscopy image shown in Figure 1b. The nonuniform deposition of polymer nanofibers creates two challenges for the air filtration technology: (1) The variation of PM removal efficiency across the whole nanofiber membrane surface. The low number density region (center of the empty space between metallic lines) would have the low efficiency of removal. (2) In order to increase the efficiency of the weakest region, it is unavoidable that more polymer fibers would need to be electrospun onto the metallic mesh support. The low fraction

Received: November 11, 2015
Revised: January 11, 2016
Published: January 20, 2016

DOI: 10.1021/acs.nanolett.5b04596
Nano Lett. 2016, 16, 1270−1275

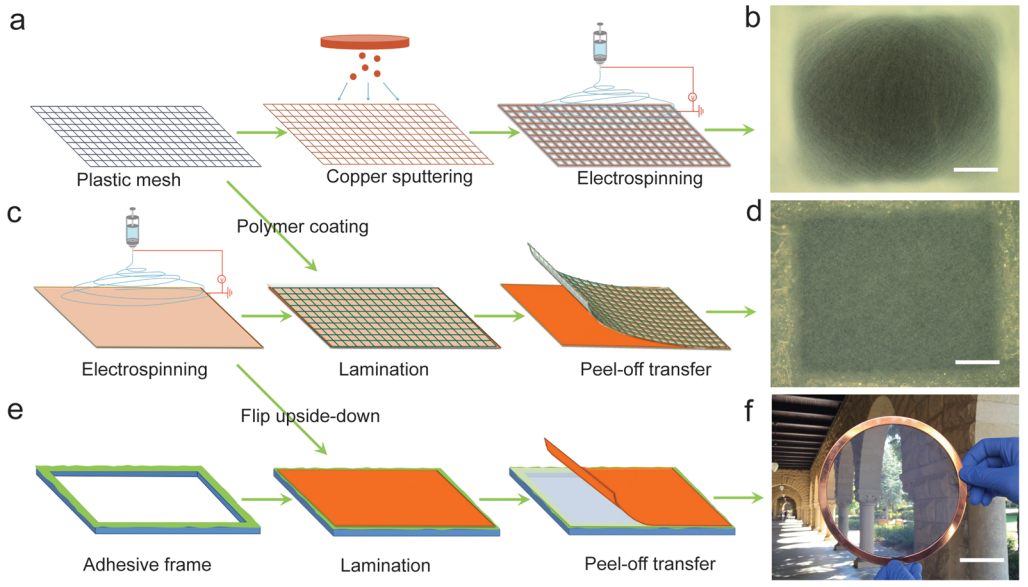

Figure 1. (a, b) Schematic showing the fabrication of transparent air filter by direct-spinning on a conductive mesh, and OM image of corresponding filter. Scale bar in b is 200 μm. (c, d) Schematic showing the fabrication of transparent air filter by transferring electrospun nanofiber film onto a plastic mesh and OM image of corresponding filter. Scale bar in c is 200 μm. (e, f) Schematic showing the transfer of freestanding electrospun nanofiber film and photograph of corresponding film. Scale bar in e is 5 cm.

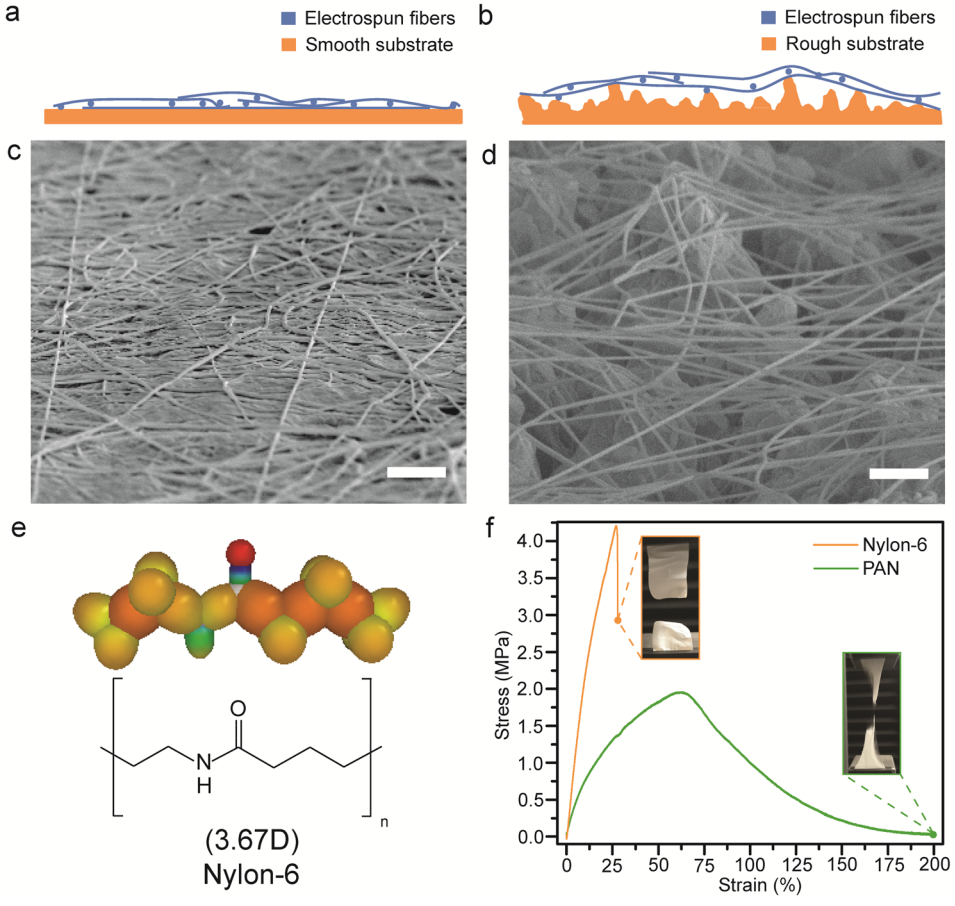

Figure 2. (a, c) Schematic and SEM image showing electrospun nanofibers on smooth copper foil. Scale bar in c is 2 μm. (b, d) Schematic and SEM image showing electrospun nanofibers on rough copper foil. Scale bar in d is 2 μm. (e) Molecular model and formula of Nylon-6 with calculated dipole moment. (f) Tensile tests of Nylon-6 and PAN electrospun nanofiber film, insets are photographs of two films at fracture point.

of nanofibers deposited onto the empty space increases electrospinning time significantly. For example, it typically takes 3 h of electrospinning in order to have filtration efficiency of ~99% for a 25 cm^2 large transparent filter. This duration is

DOI: 10.1021/acs.nanolett.5b04596
Nano Lett. 2016, 16, 1270−1275

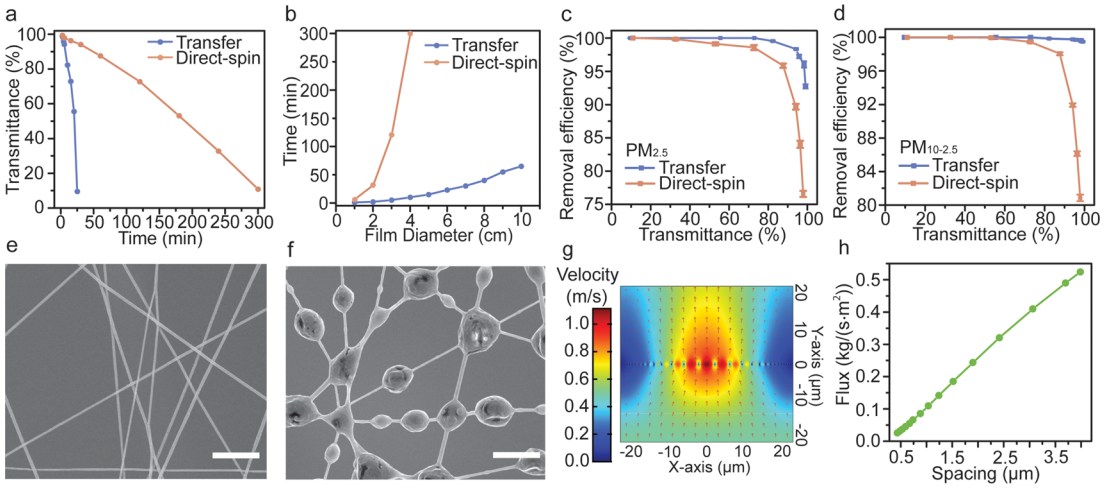

Figure 3. (a) Transmittance of filters of the same size (25 cm^2) fabricated by transfer method and direct-spin method at different electrospinning time. (b) Time required to obtain circular freestanding nanofiber films of 70% transmittance at different diameters through two methods. (c) $PM_{2.5}$ removal efficiencies of transparent filters from two methods at different transmittances. (d) $PM_{10-2.5}$ removal efficiencies of transparent filters from two methods at different transmittances. The error bar represents the standard deviation of three replicate measurements. (e, f) SEM images of Nylon-6 nanofibers before and after filtration. Scale bars in e and f are 2 μm. (g) Flow velocity field in the vicinity of an inhomogeneous nanofiber filter. Black spots represent for nanofibers with diameter of 100 nm. The air flow (0.2 m/s) comes from the bottom, and the top boundary is the outlet (1 atm). The spacing between nanofibers is sparse at the central and dense at the edge. (h) Flux at different spacing between nanofibers. Large spacing results in high flux and therefore high penetration of PM.

considered to be long when high throughput and low-cost manufacturing is desirable.

Here we developed a new fabrication process for making uniformly distributed polymer nanofibers on supported mesh with 10 times faster production speed, yet showing higher PM removal efficiency compared to our previous work[1] due to the uniform nanofiber distribution. The essential concept of our new process is based on electrospinning on a rough metallic foil collector instead of metallic mesh, followed by peel off from the foil and transfer of polymer nanofibers onto mesh. The transfer process of electrospun nanofibers is illustrated in Figure 1c, including the following series of steps: (1) Coating of the plastic mesh with the same polymer solution as the electrospun fibers. This surface coating ensures good adhesion between the fibers and the mesh. (2) Electrospinning on a rough copper foil. The rough surface morphology of the copper foil is critical to ensure a neat and complete transfer which will be discussed later. (3) Laminating the plastic mesh onto the copper foil under uniform pressure with nanofibers sandwiched in between. (4) Peeling off the plastic mesh from the copper foil with all the nanofibers transferred from the copper foil to the plastic mesh due to stronger adhesion. Compared with the nanofiber film directly electrospun onto a conductive mesh (Figure 1b), the transferred nanofiber film is much more uniform in fiber distribution as shown in optical microscopy image (Figure 1d). For electrospinning onto holey conducting mesh, the electric field concentrates around the grids,[20] so there is considerable accumulation of fibers on the grid and much less fibers across the grids. The transfer process, on the other hand, is robust such that, as we increased the mesh sizes of receiving substrate to the order of more than ten centimeters, a free-standing film of nanofiber can be peeled off and transferred. This free-standing nanofiber network can be further transferred onto substrates with nonplanar or complex geometry such as facial masks to promote their filtration efficiency. As shown in Figure 1e the steps for the transfer of free-standing nanofiber film is similar to the case of mesh transfer, except that rigid adhesive frames are used. A freestanding nanofiber film with a diameter of 15 cm is shown in Figure 1f. It is clear that the transferred nanofiber film remains its uniform distribution and no obvious defect is created.

The transfer process outlined above is now discussed in more details. Considering that the electrospun nanofiber film is actually composed of a large number of individual fibers, the transfer process becomes very unique and complex. In many works related to transfer of thin film such as ultrathin polymer film, nanowire networks, and graphene, the key is how to reduce the interaction between film and donating substrates.[21−25] However, in the case of electrospun nanofiber films, the integrity of the film is ensured by the junction points between each nanofiber. Hence, in the transfer of an electrospun nanofiber film, the challenge falls to how to maintain the film integrity by protecting the junction points between nanofibers. As shown in Figure 2a and c, the point contacts in fiber junctions is much weaker than the contact between fiber and a flat substrate due to much higher areas of interface. During the transfer process, nanofibers with much higher contact areas with the substrate will lose the junction contact with other fibers and fracture. So to prevent fiber web from fracture during transfer, the key matter is to lower the interfacial energy between fiber and substrate than that between the fiber junctions. Therefore, we choose electrodeposited copper foil with microstructures on the surface as the substrate for electrospinning to minimize the contact between the nanofiber and the substrate, as shown in Figure 2b and d.

At the same time, the selection of polymer is also critical. In our previous work, we have found that polymers with higher dipole moment such as polyacrylonitrile (PAN) have better removal efficiencies of PM particles. In this work we need to take into consideration both the chemical property of nanofibers and the mechanical property of the nanofiber films. We found Nylon-6 as a better candidate than PAN. First, as shown in Figure 2e, the dipole moment of the repeating unit in Nylon-6 is 3.67, which is very high to ensure a strong binding

DOI: 10.1021/acs.nanolett.5b04596
Nano Lett. 2016, 16, 1270−1275

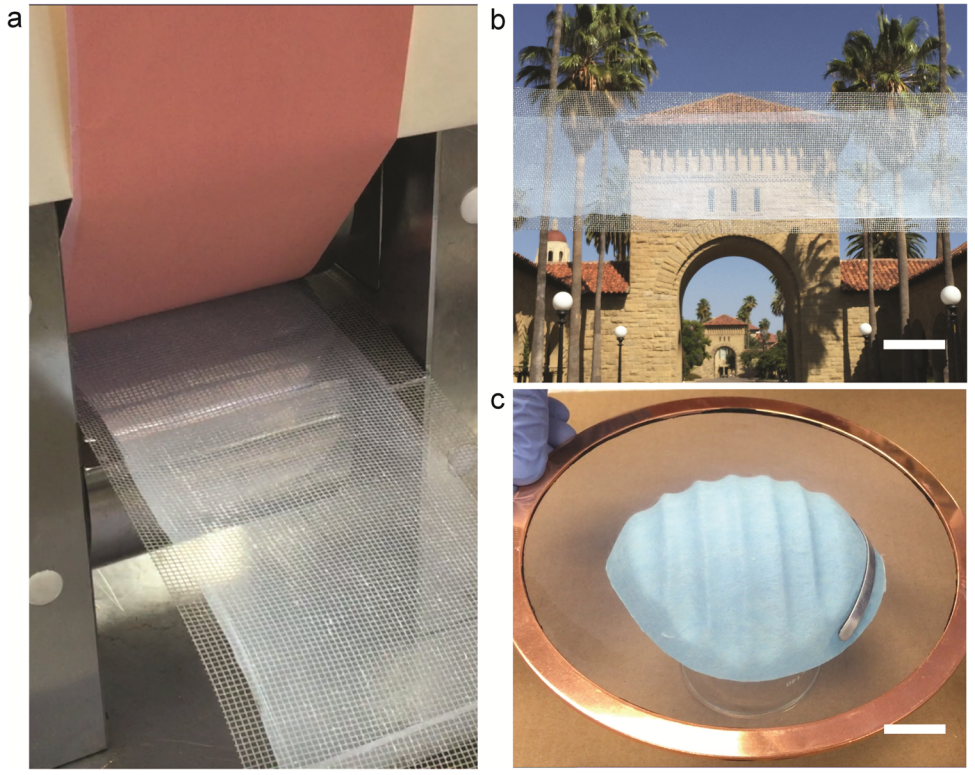

Figure 4. (a) Photograph of a roll-to-roll process to transfer electrospun nanofiber film onto plastic mesh. (b) Photograph of a roll-to-roll produced transparent air filter. The scale bar is 5 cm. (c) Photograph showing that freestanding nanofiber film can be easily transferred onto a facemask. The scale bar is 3 cm.

between nanofibers and PM particles hence a high filtration efficiency. Moreover, although the intrinsic mechanical property of bulk PAN and Nylon-6 are similar,[26,27] their nanofiber network behave very differently. Through tensile tests (Figure 2f), we can see clearly that the stress−strain curve of PAN nanofiber film diverges greatly from the counterpart of its bulk material, while Nylon-6 nanofiber film maintains an outstanding mechanical properties. The yield strength for the Nylon-6 nanofiber film is 3.65 MPa, and it exhibits very sudden fracture with little plastic deformation. In contrast, PAN nanofiber has a very low yield strength of about 0.5 MPa. We conclude that Nylon-6 nanofiber network has stronger fiber−fiber bonding, possibly due to hydrogen bonding of the amide group. Also the higher voltage required for Nylon-6 electrospinning brings branches, which can reinforce the whole structure. Insets of Figure 2f show the two kinds of nanofiber films at fracture point, indicating that PAN nanofiber film have plastic behavior that experiencing a long period of deformation during stretch and before fracture while Nylon-6 nanofiber film nearly remains elastic before fracture. The superior mechanical properties of the free-standing Nylon-6 transparent air filter is demonstrated in Movie S1 and Figure S1.

After successful transfer of electrospun nanofiber film, we fabricated air filters at different transmittance through both transfer method and direct electrospinning method to compare the process speed, scalability and filtration performance. As shown in Figure 3a, the transfer method is 10 times faster than direct-spin method to fabricate a transparent filter of the same transmittance and size (25 cm^2 in this experiment). This is because that for the direct electrospinning method most of the electrospun nanofibers are accumulated and wasted on the grid (Figure 1b) leading to a longer electrospinning time, while for the transfer method, owing to the uniform distribution of the electric field, nanofibers are distributed evenly. The transfer method can also be adopted for making free-standing nanofiber films, where the speed advantage is more obvious, shown in Figure 3b. Typically, to obtain a circular freestanding nanofiber film (70% transmittance) with a diameter of 4 cm, the direct electrospinning method onto a metal ring collector would take about 5 h, while the transfer method only needs less than 10 min. Furthermore, the direct electrospinning method on ring collector is unable to fabricate freestanding nanofiber film with diameter more than 4 cm.

We also compared the filtration efficiencies between these two different fabrication methods. It is shown that the removal efficiencies of both $PM_{2.5}$ and $PM_{10-2.5}$, are better in transferred air filters than direct-spin air filters, especially for filters with higher transmittance (Figure 3c and d). For transparent filters fabricated by transfer method, excellent capture efficiencies for $PM_{2.5}$ can be achieved for a variety of optical transmittance levels: >95.00% removal at ∼99% transmittance, >99.56% removal at ∼82% transmittance, and >99.97% removal at ∼73% transmittance for $PM_{2.5}$ capture and >99.50% removal at ∼99% transmittance for $PM_{10-2.5}$ capture. Figure 3e and f show the morphologies of Nylon-6 transparent air filter before and after PM capture. The smoke PM formed a coating layer strongly wrapped around each nanofiber.

To understand the higher filtration efficiency of filters fabricated by transfer method, we numerically solved the Navier−Stokes equations using a finite-element method (COMSOL) and obtained the flow velocity field in the vicinity of an inhomogeneous nanofiber filter. Figure 3g shows the cross section of a nanofiber array. The nanofibers lie horizontally along z-axis (out of paper), and each black spot

DOI: 10.1021/acs.nanolett.5b04596
Nano Lett. 2016, 16, 1270−1275

represents one nanofiber with diameter of 100 nm, which matches the diameter of electrospun Nylon-6 nanofibers (Figure S2). The spacing between fibers is set to be sparse at the center (4 μm) and dense at the edge (0.4 μm) to simulate the inhomogeneous nanofiber network obtained by direct electrospinning method. A constant air flow (0.2 m/s) is supplied from the bottom, and the top boundary is set to be 1 atm. The left and right sides are spatially periodic boundaries. We can see clearly that most of the flow will go through the central area, where the spacing is the largest. To further quantify this phenomenon, we integrate the velocity field in each gap, divide it with the gap length and multiply it with the air density to obtain the flux. As shown in Figure 3h, the flux increases linearly with the spacing. As a consequence, the air passing through larger spacing contribute much more to the whole air flow. Since a great amount of PM can flow through these large gaps, the overall filtration efficiency would be lower for filters with inhomogeneous spacing. This explain why filters with a non-negligible portion of large pores (direct electrospinning method) have worse efficiency than the filters with uniform spacing (transfer method) even though there are the same total amount of nanofibers per area.

In addition to capture efficiency, keeping a low air flow resistance is another important parameter to assess the performance of a filter. The pressure drops across transparent filters with different filtration efficiencies were measured. It is shown in Figure S3 that at a face velocity of 0.2 m/s, the pressure drop of a transparent air filter with a 92.73% $PM_{2.5}$ removal efficiency is just 42 Pa, and the quality factor is 0.062. For high-efficiency transparent air filter (99.56% $PM_{2.5}$ removal efficiency), the pressure drop rises to 270 Pa, which is only <0.3% of atmosphere pressure and still negligible. The quality factor of this high-efficiency transparent air filter is 0.020, which is much higher than most of the commercial high-efficiency filters. This result ensures the advantage of using natural passive ventilation to protect indoor air quality. On the basis of the real weather situation, humidity is also taken into consideration and the result is shown in Figure S4. For filters under different humidity, no obvious change in $PM_{2.5}$ removal efficiency is observed.

The fast speed and uniformity of the transfer method allow the transparent air filter to be adapted for a roll-to-roll process. As shown in Figure 4a and Movie S2, the nanofiber film is continuously transferred onto a plastic mesh screen window. Figure 4b shows the photograph of a roll-to-roll fabricated transparent air filter with the size of 50 cm long and 10 cm wide, which can act as a screen window filter in residential houses. At the same time, the transfer method can also be utilized to obtain freestanding film. As shown in Figure 4c, the freestanding film can be transferred to uneven substrate such as a facemask to promote its filtration efficiency. Besides air filtration, freestanding nanofiber film is meaningful for many other fields such as transparent electrodes,[28,29] Li-ion battery,[30] supercapacitor,[31] surface-enhanced Raman scattering (SERS)[32] and so on.

In conclusion, we have demonstrated a fast and large-scale transfer method for electrospun nanofiber film. Based on such method, we realized roll-to-roll production of transparent air filter with enhanced filtration performance and obtained freestanding nanofiber films, which can be used for commercial filter products. We believe that the large-scale transfer method will accelerate the commercialization of not only the transparent air filter but also many other applications of electrospinning.

■ ASSOCIATED CONTENT

Supporting Information

The Supporting Information is available free of charge on the ACS Publications website at DOI: 10.1021/acs.nanolett.5b04596.

Methods, pressure drop, quality factor, humidity dependent performance (PDF)

Demonstration of the strong, flexible and free-standing Nylon-6 transparent air filter (AVI)

Roll-to-roll production of transparent air filter (AVI)

■ AUTHOR INFORMATION

Corresponding Author

*E-mail: yicui@stanford.edu (Y.C.).

Author Contributions

J.X. and C.L. contributed equally to this work. J.X., C.L., P.-C.H., and Y.C. conceived and designed the experiments. J.X. fabricated the transparent air filter and measured the filtration efficiency. C.L. and P.-C.H. conducted the SEM characterization and measured the pressure drop. J.X. and P.-C.H. conducted the COMSOL simulation. P.-C.H. drew the molecular model and calculated the dipole moment. K.L., J.X., and P.-C.H. conducted the tensile tests. J.X., C.L., and Y.C. analyzed the data and cowrote the paper. All the authors discussed the whole paper.

Notes

The authors declare no competing financial interest.

■ ACKNOWLEDGMENTS

We acknowledge Stanford facilities SNL and SMF for material characterization.

■ REFERENCES

(1) Nel, A. *Science* **2005**, *309*, 1326−1326.

(2) Harrison, R. M.; Yin, J. X. *Sci. Total Environ.* **2000**, *249*, 85−101.

(3) Zhang, R.; Jing, J.; Tao, J.; Hsu, S. C.; Wang, G.; Cao, J.; Lee, C. S. L.; Zhu, L.; Chen, Z.; Zhao, Y.; Shen, Z. *Atmos. Chem. Phys.* **2013**, *13*, 7053−7074.

(4) Pope, C. A.; Dockery, D. W. *J. Air Waste Manage. Assoc.* **2006**, *56*, 709−742.

(5) Betha, R.; Behera, S. N.; Balasubramanian, R. *Environ. Sci. Technol.* **2014**, *48*, 4327−4335.

(6) Wu, S. W.; Deng, F. R.; Wei, H. Y.; Huang, J.; Wang, X.; Hao, Y.; Zheng, C. J.; Qin, Y.; Lv, H. B.; Shima, M.; Guo, X. B. *Environ. Sci. Technol.* **2014**, *48*, 3438−3448.

(7) Brook, R. D.; Rajagopalan, S.; Pope, C. A.; Brook, J. R.; Bhatnagar, A.; Diez-Roux, A. V.; Holguin, F.; Hong, Y. L.; Luepker, R. V.; Mittleman, M. A.; Peters, A.; Siscovick, D.; Smith, S. C.; Whitsel, L.; Kaufman, J. D.; Epidemiol, A. H. A. C.; Dis, C. K. C.; Metab, C. N. P. A. *Circulation* **2010**, *121*, 2331−2378.

(8) Anenberg, S. C.; Horowitz, L. W.; Tong, D. Q.; West, J. J. *Environ. Health Perspect.* **2010**, *118*, 1189−1195.

(9) Timonen, K. L.; Vanninen, E.; De Hartog, J.; Ibald-Mulli, A.; Brunekreef, B.; Gold, D. R.; Heinrich, J.; Hoek, G.; Lanki, T.; Peters, A.; Tarkiainen, T.; Tiittanen, P.; Kreyling, W.; Pekkanen, J. *J. Exposure Sci. Environ. Epidemiol.* **2006**, *16*, 332−341.

(10) Chan, C. K.; Yao, X. *Atmos. Environ.* **2008**, *42*, 1−42.

(11) Sheehan, P.; Cheng, E. J.; English, A.; Sun, F. H. *Nat. Clim. Change* **2014**, *4*, 306−309.

(12) Bruce, N.; Perez-Padilla, R.; Albalak, R. *Bull. WHO* **2000**, *78*, 1078−1092.

DOI: 10.1021/acs.nanolett.5b04596
Nano Lett. 2016, 16, 1270−1275

(13) Thavasi, V.; Singh, G.; Ramakrishna, S. *Energy Environ. Sci.* **2008**, *1*, 205−221.
(14) Faccini, M.; Vaquero, C.; Amantia, D. *J. Nanomater.* **2012**, *2012*, 1−9.
(15) Spilak, M. P.; Karottki, G. D.; Kolarik, B.; Frederiksen, M.; Loft, S.; Gunnarsen, L. *Build Environ.* **2014**, *73*, 55−63.
(16) Fisk, W. J. *Indoor Air* **2013**, *23*, 357−368.
(17) Goyal, R.; Kumar, P. *Air Qual., Atmos. Health* **2013**, *6*, 747−757.
(18) Gong, G. M.; Zhou, C.; Wu, J. T.; Jin, X.; Jiang, L. *ACS Nano* **2015**, *9*, 3721−3727.
(19) Liu, C.; Hsu, P. C.; Lee, H. W.; Ye, M.; Zheng, G. Y.; Liu, N. A.; Li, W. Y.; Cui, Y. *Nat. Commun.* **2015**, *6*, 6205.
(20) Li, D.; Wang, Y. L.; Xia, Y. N. *Nano Lett.* **2003**, *3*, 1167−1171.
(21) Baxamusa, S. H.; Stadermann, M.; Aracne-Ruddle, C.; Nelson, A. J.; Chea, M.; Li, S. L.; Youngblood, K.; Suratwala, T. I. *Langmuir* **2014**, *30*, 5126−5132.
(22) Bae, S.; Kim, H.; Lee, Y.; Xu, X. F.; Park, J. S.; Zheng, Y.; Balakrishnan, J.; Lei, T.; Kim, H. R.; Song, Y. I.; Kim, Y. J.; Kim, K. S.; Ozyilmaz, B.; Ahn, J. H.; Hong, B. H.; Iijima, S. *Nat. Nanotechnol.* **2010**, *5*, 574−578.
(23) Gao, L. B.; Ni, G. X.; Liu, Y. P.; Liu, B.; Castro Neto, A. H.; Loh, K. P. *Nature* **2013**, *505*, 190−194.
(24) Lee, Y.; Bae, S.; Jang, H.; Jang, S.; Zhu, S. E.; Sim, S. H.; Song, Y. I.; Hong, B. H.; Ahn, J. H. *Nano Lett.* **2010**, *10*, 490−493.
(25) Madaria, A. R.; Kumar, A.; Ishikawa, F. N.; Zhou, C. *Nano Res.* **2010**, *3*, 564−573.
(26) Hinrichs, G. *J. Polym. Sci. Polym. Sym.* **1972**, *1*, 303−314.
(27) Penel-Pierron, L.; Seguela, R.; Lefebvre, J. M.; Miri, V.; Depecker, C.; Jutigny, M.; Pabiot, J. *J. Polym. Sci., Part B: Polym. Phys.* **2001**, *39*, 1224−1236.
(28) Hsu, P. C.; Wang, S.; Wu, H.; Narasimhan, V. K.; Kong, D. S.; Ryoung Lee, H.; Cui, Y. *Nat. Commun.* **2013**, *4*, 2522.
(29) Wu, H.; Kong, D. S.; Ruan, Z. C.; Hsu, P. C.; Wang, S.; Yu, Z. F.; Carney, T. J.; Hu, L. B.; Fan, S. H.; Cui, Y. *Nat. Nanotechnol.* **2013**, *8*, 421−425.
(30) Zhang, B. A.; Yu, Y.; Huang, Z. D.; He, Y. B.; Jang, D.; Yoon, W. S.; Mai, Y. W.; Kang, F. Y.; Kim, J. K. *Energy Environ. Sci.* **2012**, *5*, 9895−9902.
(31) Wu, Q.; Xu, Y. X.; Yao, Z. Y.; Liu, A. R.; Shi, G. Q. *ACS Nano* **2010**, *4*, 1963−1970.
(32) He, D.; Hu, B.; Yao, Q. F.; Wang, K.; Yu, S. H. *ACS Nano* **2009**, *3*, 3993−4002.

DOI: 10.1021/acs.nanolett.5b04596
Nano Lett. 2016, 16, 1270−1275